Construction of a Multifunctional Enzyme Complex via the Strain-Promoted Azide−Alkyne Cycloaddition

Sanne Schoffelen,[†] Jules Beekwilder,[‡] Marjoke F. Debets,[†] Dirk Bosch,[‡] and Jan C. M. van Hest*[,†]

[†]Department of Bio-organic Chemistry, Radboud University Nijmegen, Heyendaalseweg 135, 6525 AJ Nijmegen, The Netherlands
[‡]Plant Research International, Wageningen University and Research Centre, Droevendaalsesteeg 1, 6708 PB Wageningen, The Netherlands

Ⓢ *Supporting Information*

ABSTRACT: Inspired by the multienzyme complexes occurring in nature, enzymes have been brought together *in vitro* as well. We report a co-localization strategy milder than nonspecific cross-linking, and free of any scaffold and affinity tags. Using non-natural amino acid incorporation, two heterobifunctional linkers, and the strain-promoted azide−alkyne cycloaddition as conjugation reaction, three metabolic enzymes are linked together in a controlled manner. Conjugate formation was demonstrated by size-exclusion chromatography and gel electrophoresis. The multienzyme complexes were further characterized by native mass spectrometry. It was shown that the complexes catalyzed the three-step biosynthesis of piceid *in vitro* with comparable kinetic behavior to the uncoupled enzymes. The approach is envisioned to have high potential for various biotechnological applications, in which multiple biocatalysts collaborate at low concentrations, in which diffusion may be limited and/or side-reactions are prone to occur.
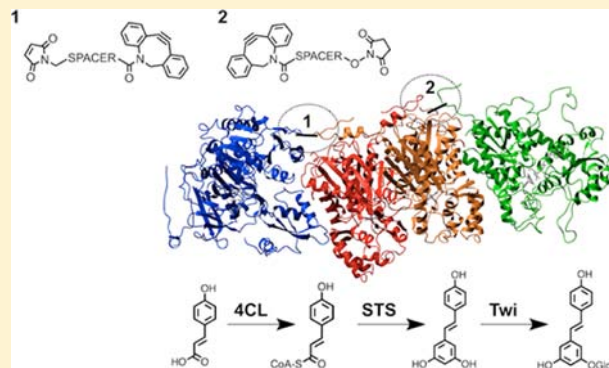
INTRODUCTION

Metabolic channeling plays an important role in the biosynthesis of numerous natural products.[1,2] Through the spatial organization of enzymes involved in metabolic cascade reactions, intermediates are transferred from one catalytic site to the other without or with less diffusion into the bulk phase of the cell. This phenomenon has inspired researchers to bring together enzymes in an artificial way as well.[3,4] Such synthetic enzyme complexes are considered to be a promising tool for biotechnological applications in which accelerated reaction rates and a decrease of potential metabolite degradation are desired.[5]

Several strategies for the *in vitro* co-localization of enzymes have been reported. These include nonspecific co-immobilization, noncovalent encapsulation, the construction of gene fusions, and scaffold-mediated co-localization.[6] Combined cross-linked enzyme aggregates (so-called combi-CLEAs) have been shown to be a straightforward way for the co-immobilization of multiple biocatalysts without the need of any solid support.[7−9] However, the low degree of specificity of the method, in which a random number of lysine residues is targeted in each protein molecule, may lead to (partial) inactivation of the enzymes. The creation of gene fusions is a highly controlled and thus attractive alternative. However, the proteins can only be linked *via* their N- or C-termini. Moreover, when coupling more than two biocatalysts, proper folding of the multicatalytic polypeptide chain becomes highly challenging. A very elegant approach is the scaffold-mediated

co-localization.[10−17] Yet, the use of a scaffold such as DNA, RNA, or the scaffoldin protein of the cellulosome requires the introduction of affinity tags in the enzyme and the addition of a potentially undesirable, extra component (the scaffold) to the system.

Here, we describe a strategy for the construction of a synthetic multienzyme complex which is free of any scaffold and affinity tags, while the control over the assembly formation is retained. Three metabolic enzymes are linked to each other using two heterotelechelic linkers and the strain-promoted azide−alkyne cycloaddition as bioconjugation method. Recently, the copper-free click reaction has been applied for the synthesis of bispecific antibodies and antibody−protein conjugates.[18−21] However, to our knowledge this is the first example in which this highly efficient reaction is applied to couple multiple enzyme molecules, in this way producing a so-called synthetic metabolon.

The synthesis and glycosylation of resveratrol was selected as model system. Resveratrol (trans-3,5,4′-trihydroxystilbene) is a polyphenol produced by specific plants such as the grapevine, the peanut, the olive tree, and the cranberry plant. Recently, the compound has received a lot of attention for its potential medicinal properties, such as antioxidative and anticarcinogenic activity, as well as protection against cardiovascular dis-

Scheme 1. Biosynthesis and Glycosylation of Resveratrol
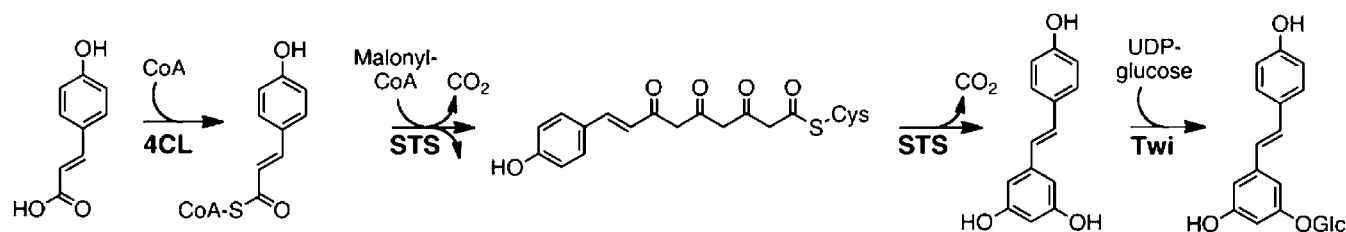
eases.[22,23] Resveratrol is derived from *para*-coumaric acid, which is attached to coenzyme A (CoA) by the action of 4-coumarate:coenzyme A ligase (4CL, EC 6.2.1.12). Subsequently, three acetyl units (derived from malonyl-CoA) are added to coumaroyl-CoA followed by a cyclization reaction, all catalyzed by stilbene synthase (STS, EC 2.3.1.95). Coexpression of 4CL and STS has facilitated the biosynthesis of resveratrol in microorganisms.[24−26] Moreover, a 4CL:STS fusion protein has been produced for the production of resveratrol in *Saccharomyces cerevisiae* and human HEK293 kidney cells.[27]

One of the most abundant resveratrol derivatives is the glucoside piceid (*trans*-resveratrol-3-*O*-β-glucoside). In general, glycosylation of small organic compounds is known to be advantageous. Increased water-solubility leads to improvements in downstream processing and/or better bio- and pharmacological properties.[28] With respect to flavonoids, a class of plant phenols related to resveratrol, it has been suggested that glycosylation leads to more efficient absorption in the small intestine when compared to the corresponding aglycon.[29,30] Therefore, in the present study we aimed at constructing a multienzyme complex not only consisting of 4CL and STS but also containing the UDP-glucosyltransferase Twi (EC 2.4.1.35). This would enable the biosynthesis and subsequent glycosylation of resveratrol by one multienzyme complex as depicted in Scheme 1.

■ EXPERIMENTAL SECTION

General Materials and Methods. Primers were purchased from Biolegio (Malden, The Netherlands) and dNTP mix from Invitrogen. Restriction enzymes were from New England Biolabs and Promega. Natural amino acids, kanamycin, lysozyme, PMSF, imidazole, dithiothreitol (DTT), coenzyme A (CoA), malonyl-CoA, resveratrol, and UDP-glucose were obtained from Sigma Aldrich. Azidohomoalanine was prepared as described previously.[31] Ampicillin and IPTG were purchased from MP Biomedicals, and thiamine and glucose from Merck. Heterotelechelic linkers **1** and **2** were synthesized as described in the Supporting Information. *p*-Coumaric acid was from Janssen Pharmaceutica and piceid from Extrasynthese. 2xYT medium was provided by the Nijmegen Centre for Molecular Life Sciences (NCMLS, The Netherlands). Solutions used for protein expression were sterilized by autoclave or by filtration over a 0.2 μm membrane (Corning Life Sciences, or Whatman GmbH). Phosphate buffer contained 25 mM NaH_2PO_4 and 100 mM NaCl (pH 7.5). Ultrapure Milli-Q water (MQ) was purified using a WaterPro PS polisher (Labconco, Kansas City, MO) set to 18.2 MΩ/cm. 10 kDa MWCO centrifugal filter units (Millipore) were used for ultrafiltration. Centrifugation was performed on a Biofuge Pico microcentrifuge (Heraeus Instruments), a Multifuge 3 S-R (Heraeus Instruments) using a Sorvall Heraeus 75006445 rotor, a RC-5 Superspeed

Refrigerated centrifuge (Sorvall, Dupont Instruments) using a GS-3 or SM-24 rotor and a Sepatech Minifuge RF (Heraeus Instruments) with a #3360 rotor. Cell cultures were shaken at 200 rpm in an Infors HT Multitron shaker. Cell densities were measured on an Ultrospec 10 Cell density meter (Amersham Biosciences). Conjugation reactions as well as enzyme activity assays were shaken on an Eppendorf Thermomixer comfort.

Plasmid Construction. The genes encoding for 4CL2 from *Nicotiana tabacum* (GenBank accession no. U50846) and STS from *Vitis vinifera* (GenBank accession no. EU156062) were amplified from pACYCDuet-4CL2/STS (vector from Novagen, plasmid provided by Plant Research International, The Netherlands) using the following primers (restriction sites in italics): Forward *Bam*HI-4CL: ATAT *GGATCC* ATG GAG AAA GAT ACA AAA CAG G; Reverse *Hind*III-4CL: ATAT *AAGCTT* TTA ATT TGG AAG CCC AGC AGC; Forward *Bam*HI-STS: ATAT *GGATCC* ATG GCT TCA GTC GAG GAA ATT AG; Reverse *Hind*III-STS: ATAT *AAGCTT* TTA ATT TGT AAC CAT AGG AAT GC. The reaction mixture (50 μL) contained 200 pmol of each primer, Advantage cDNA polymerase mix (1 μL, Clontech), dNTP mix (0.2 mM of each), 5 μL template DNA (100 times diluted), and 10× reaction buffer (5 μL). PCR was conducted on a PE Applied Biosystem 9700 thermal cycler under the following conditions: 95 °C for 2 min followed by 30 cycles of (95 °C for 30 s, 55 °C for 30 s, 68 °C for 90 s) and finally 4 °C for 5 min. The PCR amplified fragments were purified from an agarose gel using the Qiagen Gel Extraction kit. DNA fragments were treated with *Bam*HI and *Hind*III and inserted in expression vector pQE30 (Qiagen), which contains an N-terminal histidine tag. Following ligation and transformation, plasmids pQE30−4CL and pQE30-STS were obtained by isolation from XL-Blue1 *E. coli* cells.

Enzyme Production, Purification, and Characterization. Methionine auxotrophic *E. coli* MTD123[32,33] cells were co-transformed with repressor plasmid pREP4 (Qiagen) and pQE30-4CL or pQE30-STS. *E. coli* BLR(DE3) cells (Novagen) were transformed with pAC-TC32 (provided by PRI, The Netherlands), containing the gene encoding for glucosyl transferase Twi from *Solanum lycopersicm* (GenBank accession no. CAA59450.1) downstream of a histidine tag. 2x YT medium supplemented with the required antibiotics was inoculated with a single colony and incubated overnight at 37 °C. The overnight culture was diluted in fresh 2x YT medium to an OD_{600} of 0.1 and grown at 37 °C. When an OD_{600} of 0.8 was reached, isopropyl-β-D-thiogalactopyranoside (IPTG) was added to a final concentration of 1 mM. Protein production was allowed to take place for 20 h at 18 °C. STS containing azidohomoalanine (AHA-STS) was prepared by resuspending cells from an overnight culture in M9 minimal medium containing all natural amino acids. When an OD_{600} of 0.6 was reached, the culture was sedimented by centrifugation, washed

twice with cold 0.9% NaCl, and resuspended in M9 minimal medium containing all natural amino acids except for methionine. After incubation for 10 min at 37 °C, azidohomoalanine (40 mg/L) and IPTG (1 mM) were added followed by overnight incubation at 18 °C.

All three His$_6$-tagged enzymes were purified by Ni^{2+} NTA affinity chromatography under native conditions (Qiagen). The bacteria pellet was lysed by incubation at 4 °C for 30 min in lysis buffer (30 mL of 50 mM NaH$_2$PO$_4$, 300 mM NaCl, 10 mM imidazole, pH 8.0) containing PMSF as protease inhibitor (1 mM) and lysozyme (1 mg/mL). After sonication for at maximum 5 min (40% duty cycle, power 6) the lysate was cleared by centrifugation at 4 °C (13 000 g, 30 min). The proteins were allowed to bind to Ni^{2+} NTA beads (1 mL, Qiagen) for 2 h at 4 °C. Beads were loaded on a column, which was washed once with lysis buffer and twice with wash buffer (two times 10 volumes of 50 mM NaH$_2$PO$_4$, 300 mM NaCl, 20 mM imidazole, pH 8.0). Enzymes were eluted in elution buffer (10 mL of 50 mM NaH$_2$PO$_4$, 300 mM NaCl, 250 mM imidazole, pH 8.0). As for STS, 20 mM 2-mercaptoethanol was added to lysis buffer, wash buffer, and elution buffer.

Elution fractions containing the enzymes were concentrated by centrifugation at 4 °C using an Amicon Ultra-15 Centrifugal Filter Device (10 000 NMWL). Further purification was performed by size exclusion chromatography using a Superdex 75 PC 10/300 column on an ÄKTA FPLC (GE Healthcare Life Sciences). Both column and fraction collector were kept at 4 °C. Phosphate buffer (25 mM NaH$_2$PO$_4$ and 100 mM NaCl, pH 7.5) was used as eluent while applying a flow rate of 0.5 mL/min and collecting 0.5 mL fractions. Glycerol was added to a final concentration of 10% and aliquots were snap-frozen and stored at −20 °C until use.

Purity was checked by gel electrophoresis. Protein concentrations were determined by measuring absorbance at 280 nm on a Nanodrop ND-1000 spectrometer. Extinction coefficients were used as determined by the "Protein Calculator v 3.3" at http://www.scripps.edu/~cdputnam/protcalc.html, being 0.45, 0.90, and 1.25 (mg/mL)$^{-1}$ cm^{-1} for 4CL, STS, and Twi, respectively.

Modification of AHA-STS with PEG2000-Dibac and Cbz-Dibac. Two or 20 equiv of PEG2000-Dibac (1 or 10 mM stock in MQ) was added to AHA-STS. Samples were incubated for 16 h at room temperature while being gently shaken, and analyzed by gel electrophoresis using a 7.5% polyacrylamide gel. Alternatively, 5 equiv of Cbz-Dibac (5 mM stock in DMSO) were allowed to react with AHA-STS (2 mg/mL) for 2 h at room temperature. An excess of azidohomoalanine was added to quench the labeling reaction and reagents were removed by ultrafiltration. The product was treated with trypsin and analyzed by LC-MS (see Supporting Information).

Modification of 4CL with PEG2000-maleimide, N-(2-aminoethyl)maleimide, and Linker 1. 1, 2, and 10 equiv of methoxypolyethylene glycol maleimide (Sigma Aldrich, average M_n 2000) were allowed to react with 4CL (1 mg/mL in phosphate buffer, pH 7) for 2 h at room temperature. For analysis on a 7.5% polyacrylamide gel, sample buffer with 2-mercaptoethanol was added which quenched the reaction. For activity analysis, an aliquot of the reaction product was diluted 20 times, of which 2 μL was added to the activity assay mixture. Additionally, 4CL (2 mg/mL in phosphate buffer, pH 7) was reacted with 2 and 10 equiv of 1 or N-(2-aminoethyl)maleimide (2 or 10 mM stock solution in DMSO). The final concentration of DMSO was 8%. After shaking for two hours

at room temperature, the reactions were quenched by addition of an excess of DTT. The excess of maleimide-containing molecule and DTT was removed by ultrafiltration using phosphate buffer. An aliquot of the reaction product was diluted 20 times, of which 2 μL was added to the activity assay mixture. In order to determine the degree and site of labeling, the remaining modified 4CL was analyzed by mass spectrometry, before and after treatment with trypsin, as described in the Supporting Information.

Modification of Twi with Linker 2. Twi (2−4 mg/mL in phosphate buffer, pH 7.5) was reacted with 1, 2, 5, or 10 equiv of 2 (stock solutions in DMSO) for 2 h while being shaken at room temperature. The final concentration of DMSO never exceeded 10%. Excess of linker was removed by ultrafiltration. An aliquot equal to 2 μg of the reaction product was used for activity analysis. The degree of labeling was determined by mass spectrometry under native conditions only.

Production of Enzyme Conjugates. *One-Step Approach.* 4CL-1 and Twi-2 were prepared as described above using 2 equiv of 1 and 10 equiv of 2 relative to 4CL and Twi, respectively. Excess of linker was removed by ultrafiltration at 4 °C (3 times 450 μL phosphate buffer was added). Subsequently, 170 μg of 4CL-1 and 150 μg of Twi-2 were added to 125 μg AHA-STS resulting in a molar ratio of 1:1:1 for 4CL:STS:Twi. Glycerol and DTT were added to a final concentration of 10% and 5 mM, respectively. After overnight incubation at room temperature, enzyme conjugates were purified over a Superdex200 PC 3.2/30 column (GE Healthcare Life Sciences) on a SMART FPLC (Amersham Pharmacia). Phosphate buffer was used as eluent while applying a flow rate of 40 μL/min and collecting 40 μL fractions. For analysis by gel electrophoresis (7.5% polyacrylamide), fractions eluting at 1.08−1.24 mL, 1.32−1.40 mL, and 1.48−1.56 mL were collected. SDS and 2-mercaptoethanol were omitted from the gel solution and sample buffer when running the gel under native conditions. Individual fractions were analyzed by native mass spectrometry as described in the Supporting Information.

Two-Step Approach. 4CL-1 was prepared according to the previously described procedure using 2 equiv of 1. Excess of linker was removed by ultrafiltration at 4 °C (3 times 450 μL phosphate buffer was added). 225 μg of AHA-STS was added to 155 μg of 4CL-1 resulting in a molar ratio of 2:1 for STS:4CL, and a final reaction volume of 75 μL. After incubation at room temperature for 5 h, the reaction product was concentrated to less than 50 μL using a centrifugal filter unit and injected on a Superdex200 PC 3.2/30 column. The fractions containing the 4CL-STS dimer were pooled and concentrated to 30 μL. The amount of 4CL-STS dimer was deduced from the size-exclusion chromatogram. A 3-fold molar excess of Twi-2 was added together with glycerol to a final concentration of 10%. After incubation at room temperature for 12 h the reaction product was reinjected on a Superdex200 PC 3.2/30 column.

4CL-STS and Twi-STS. The effect of conjugation on the individual enzymes was determined by preparing 4CL-STS and Twi-STS complexes. 4CL-1 and Twi-2 were prepared as previously described and reacted separately with AHA-STS in a 1:1 molar ratio. Conjugation was allowed to take place for 5−6 h at room temperature. Uncoupled enzymes were separated from the X-STS:STS and X-STS:STS-X complexes (X = 4CL or Twi) by size-exclusion chromatography.

Enzyme Activity Assays. All enzyme activity assays were carried out in a buffered solution containing 25 mM NaH$_2$PO$_4$

and 100 mM NaCl (pH 7.5). Stock solutions of Coenzyme A and UDP-glucose (each 10 mM in MQ) were stored in aliquots at −20 °C and thawed upon use. Stock solutions containing 10 mM *para*-coumaric acid in EtOH, 0.5 or 10 mM malonyl-CoA in MQ, and 5 mM resveratrol in EtOH were stored at −20 °C as well. Time samples of STS and Twi activity assays were analyzed by high-performance liquid chromatography (HPLC) on a Shimadzu analytical HPLC over a C18 column. 20 μL was injected. A linear gradient was applied from 5% acetonitrile in MQ/0.1% trifluoroacetic acid to 50% acetonitrile in MQ/0.1% trifluoroacetic acid in 30 min. Compounds were detected by measuring absorbance at 307 nm. Calibration curves were generated using commercially available resveratrol and piceid.

4CL. Formation of coumaroyl-CoA was followed in time at 30 °C by measuring absorbance at 355 nm in a Multicounter Wallac Victor[2] plate reader (PerkinElmer Life Sciences). The reaction mixture consisted of 0.1 mM CoA, 0.05 mM *para*-coumaric acid, 3.125 mM ATP, 3.125 mM MgCl$_2$, and 1.25 mM DTT in 200 μL. ATP was added as last component to start the reaction. The slope of the curve obtained during the first two minutes was taken as a measure for activity.

STS. The specific activity of Met-STS and AHA-STS was determined at relatively high substrate concentrations, i.e., 0.5 mM malonyl-CoA and 0.1 mM coumaroyl-CoA. The amount of resveratrol formed at 30 °C by 2 μg of enzyme in 100 μL was measured. Coumaroyl-CoA was prepared using 4CL. The 4CL assay reaction mixture containing 0.5 mM *para*-coumaric acid and 1 mM CoA was incubated at 30 °C until full conversion was observed by UV/vis spectroscopy. An aliquot of this solution was diluted in buffer containing the required amounts of malonyl-CoA and STS. After quenching a 25 μL aliquot with 12.5 μL 50% acetic acid, the product was extracted using 150 μL EtOAc. The organic phase was collected and the solvent was removed by speedvac, after which the product was redissolved in 50 μL 50% MeOH in MQ/5% formic acid and analyzed by HPLC. STS activity exhibited by the conjugates was determined using an assay mixture containing 25 μM coumaroyl-CoA, 0.4 mM malonyl-CoA, and an enzyme concentration of around 0.4 μM (2 μg per 100 μL). Reactions were incubated at 30 °C. Aliquots were quenched at three different time points by addition of 50% acetic acid and analyzed by HPLC after extraction with EtOAc.

Twi. Glycosylation activity displayed by modified Twi and the conjugates was measured in a reaction mixture containing 25 μM resveratrol, 2 mM UDP-glucose, and an enzyme concentration of around 0.2 μM (1 μg per 100 μL) Twi. All time samples were quenched by the addition of 10% formic acid in MeOH (25 μL was added to a 25 μL aliquot of the reaction) and analyzed by HPLC.

The three-enzyme cascade reaction was followed in time at 30 °C using a phosphate buffered solution containing 25 μM *para*-coumaric acid, 25 μM coenzyme A, 100 μM malonyl-CoA, and 200 μM UDP-glucose. The amount of conjugate or uncoupled enzymes added to the assay mixture was adjusted in such a way that the individual enzyme activities were equal. Aliquots were quenched at given time points with one volume of 10% formic acid in MeOH, and analyzed by HPLC.

For determination of the effect of conjugation on the individual enzyme activities, the area under the size-exclusion chromatogram recorded by measuring absorbance at 280 nm was taken as a measure for the total amount of protein in each fraction. The sum of the molar extinction coefficients of the separate enzymes was used as the molar extinction coefficient

of the conjugates: $\varepsilon_{X\text{-STS:STS}} = 2 * \varepsilon_{STS} + 1 * \varepsilon_X$ and $\varepsilon_{X\text{-STS:STS-X}} = 2 * \varepsilon_{STS} + 2 * \varepsilon_X$ in which X is 4CL or Twi. These were used to calculate the (apparent) molar amount of each enzyme in the conjugate fractions. As for the uncoupled enzyme fraction, the relative amounts of STS and X were determined by measuring the intensity of the individual bands on a Coomassie-stained SDS-PAGE gel using an Odyssey imaging system and *ImageJ* software. This information was used to calculate an apparent molar extinction coefficient, which was subsequently used to calculate the (apparent) molar amounts of each enzyme in the uncoupled enzyme fraction. The detected enzyme activity in each fraction was divided by the (apparent) molar amount of the respective enzyme used in the assay. The value thus obtained from the uncoupled enzyme fraction was set at 100%.
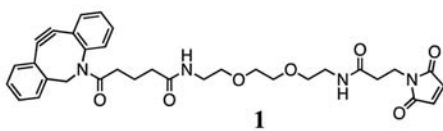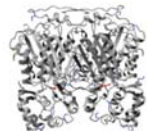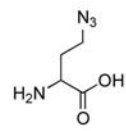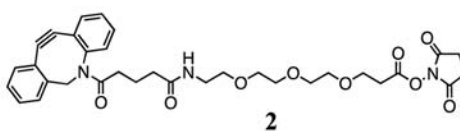
■ RESULTS

Selection of Modification Strategies and Heterotelechelic Linkers. Linkage of the three enzymes *via* the strain-promoted azide−alkyne cycloaddition required functionalization of the proteins with an azide or cyclooctyne moiety. The modification strategies that were selected for introduction of these functional handles are depicted in Table 1.

In the past, we have shown that the residue-specific replacement of methionine by azidohomoalanine can be used for site-specific modification of enzymes.[31] Here, this strategy was selected for functionalization of STS, which contained the smallest number of methionine residues. This was considered to be relevant, as it was expected that protein expression in the presence of the non-natural amino acid would become more challenging with an increasing number of methionine codons. Second, heterotelechelic linker **1** was designed to introduce a dibenzocyclooctyne moiety in 4CL *via* a cysteine-maleimide coupling. This choice was based on the homology model of 4CL showing the low solvent accessibility of the cysteine residues. The low abundance of cysteine as naturally occurring reactive amino acid made this modification strategy to be the preferred method for Twi as well. However, it was found that Twi became inactive when treated with maleimide. The solvent accessibility of cysteine residue 298, which is located in the binding region of the donor UDP glucose, was hypothesized to be the reason for this. As specific modification strategies involving chemical reagents (such as pyridoxal 5′-phosphate or the diazotransfer reagent for N-terminal specific modification) were found to result in enzyme precipitation and/or inactivation, it was decided to target the amine functionalities instead, using the *N*-hydroxysuccinimide (NHS) ester containing linker **2**. In both linkers a short ethylene glycol spacer was inserted to allow for flexibility in the final multienzyme assemblies.

Incorporation of Azidohomoalanine in Stilbene Synthase. STS was expressed in the presence of azidohomoalanine (AHA). The mass detected for AHA-STS showed that the incorporation of the nonproteinogenic amino acid was successful. Compared to STS containing methionine (Met-STS), a decrease in mass was found that corresponded to the expected 11 methionine-azidohomoalanine replacements. Based on the relative abundance of the tryptic fragments containing either AHA or Met, the degree of AHA incorporation was 90% (see Supporting Information Figure S1). The influence of AHA incorporation on activity was determined by comparing the initial velocities of AHA-STS and Met-STS. With respect to AHA-STS, values were found varying

Table 1. Modification Strategies Used to Functionalize 4CL, STS, and Twi for Subsequent Conjugation *via* the Strain-Promoted Azide–Alkyne Cycloaddition

enzyme	functional target	bioconjugate reagent / strategy
4CL	cysteine	maleimide coupling
STS	methionine	replacement by azidohomoalanine
Twi	N-terminus / lysine	*N*-hydroxysuccinimide coupling

from 0.24 to 0.33 nmol/s/mg enzyme. Values observed for Met-STS varied between 0.30 and 0.60 nmol/s/mg. So, replacement of methionine still yielded a functional enzyme, albeit with somewhat lower activity. Like other type III polyketide synthases, STS is known to form a dimer.[34] According to our homology model, methionine residue 170 is located at the dimerization interface. Moreover, methionine residue 149 points toward the active site. It was hypothesized that the replacement of one of these methionine residues by AHA somehow affected the catalytic activity. Site-directed mutagenesis of the respective residues might prevent this. However, this was considered to be outside the scope of our research. Importantly, the K_m toward coumaroyl-CoA was shown to be unaffected.

The accessibility of the azide residues was addressed by incubation of the protein with polyethylene glycol functionalized with a dibenzoazacyclooctyne moiety (PEG-Dibac, M_n 2000).[35] The reaction product was analyzed by gel electrophoresis. Up to four polymer chains were attached to the enzyme, as deduced from the additional bands that were visible on the polyacrylamide gel (see Figure 1A). Based on the homology model of the STS dimer (see Figure 1B), the four most N-terminal AHA residues (1, 13, 61, and 76) as well as residue 99 and 401 were expected to be solvent accessible. To verify whether these were the reactive residues, AHA-STS was incubated with carboxybenzyl-protected dibenzoazacyclooctyne (Cbz-Dibac). The reaction product was treated with trypsin and analyzed by mass spectrometry. Masses corresponding to the tryptic fragments harboring residues 1, 13, 61, and 76 modified with Cbz-Dibac were detected (see Supporting Information Figure S1, D and E). As for the tryptic fragments
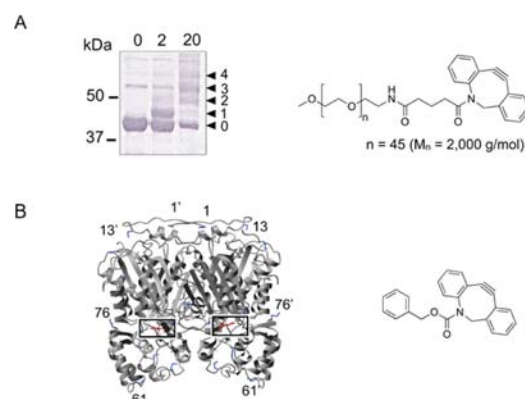

Figure 1. Accessibility of the azide moieties in AHA-STS. (A) Pegylation of AHA-STS using PEG-Dibac; see structure on the right, analyzed by gel electrophoresis. The numbers above the gel indicate the molar equivalents of PEG added relative to STS. The numbers and arrows at the right side point out the number of PEG chains attached to the enzyme. (B) Homology model of the STS dimer and structure of Cbz-Dibac, used to assess the accessibility of azide residues. The two active sites are surrounded by black boxes, and the solvent accessible methionine residues are indicated by numbers.

containing residues 99 and 401, masses of the unlabeled species were found to be present. The degree of labeling varied per residue. For example, tryptic fragment #3–20 was fully labeled, whereas both unreacted and reacted species were detected for tryptic fragments #58–65 and #75–78.

Site-Specific Functionalization of 4-Coumarate:coenzyme A Ligase. The accessibility of the ten cysteines in 4CL was assessed by incubation with α-methoxy-poly(ethylene

glycol)-*ω*-maleimide (PEG-maleimide, M_n 2000). To our delight, only one single product was detected by gel electrophoresis, even when 10 equiv of the maleimide was added (see Figure 2A). Moreover, the activity of the enzyme
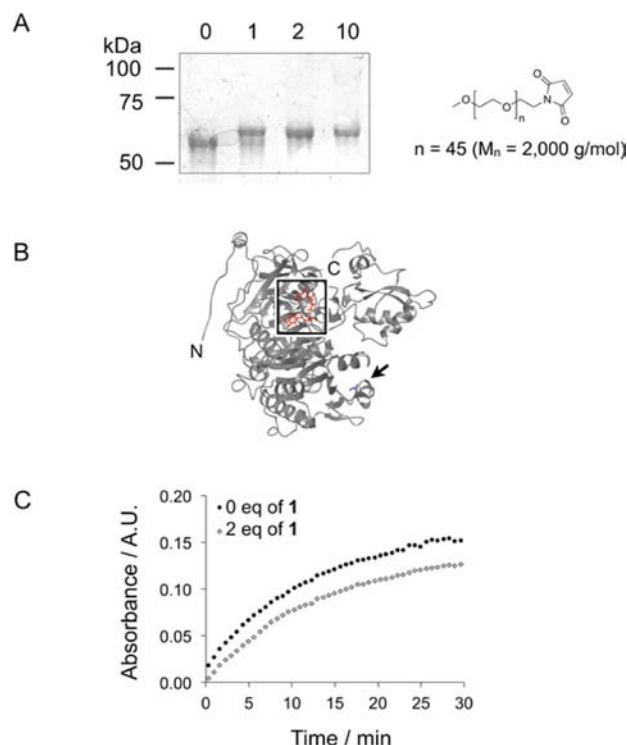

Figure 2. Monofunctionalization of 4CL *via* the single accessible cysteine residue 145. (A) Pegylation of 4CL using maleimide-PEG analyzed by gel electrophoresis (7.5% polyacrylamide). The numbers above the gel indicate the molar equivalents of PEG added relative to 4CL. (B) Homology model of 4CL. Cysteine 145 is pointed out by the arrow, the active site is surrounded by the black box, and the N- and C-termini are indicated by N and C, respectively. (C) Effect of the linkage of **1** on 4CL activity. The formation of coumaroyl-CoA was followed in time by monitoring the absorbance at 355 nm. The initial slope was taken as a measure for the activity.

was entirely retained. In order to identify the reactive cysteine, a proteolytic digest of the modified enzyme was analyzed by LC-MS. The tryptic fragment corresponding to residues 139–149 was shifted in mass when reacted with different maleimide-containing molecules (see Supporting Information Figure S2). The homology model based on 4CL from *Populus tomentosa* supported this observation, showing that Cys-145 is freely accessible, located on the top of a turn (see Figure 2B). The other cysteines are buried inside the protein except for Cys-163 and Cys-171. However, these residues at the surface of the enzyme are close to each other and it is expected that they form a sulfur bridge in the absence of a reducing agent.

To enable linkage to STS, 4CL was incubated with heterotelechelic linker **1**. Incubation of 4CL with 2 equiv of **1** resulted in monofunctionalized enzyme as determined by mass spectrometry. Again, the activity was conserved, though slightly decreased to 80% when compared to unfunctionalized enzyme (see Figure 2C). Remarkably, contrary to what was observed when using PEG-maleimide, a 10-fold excess of **1** relative to protein led to difunctionalized, inactive enzyme. Clearly, at this elevated concentration of **1**, a less accessible cysteine, crucial to the catalytic activity of the enzyme, had reacted as well. Overall,

it can be stated that 4CL could be site-specifically modified via Cys-145 using a small excess of maleimide while the majority of its activity was retained.

Selective Modification of UDP-Glucosyl Transferase Twi. Twi contains 32 amine groups of which ideally only one would be modified with linker **2**. In order to find the optimal conditions for selective modification, the enzyme was reacted with an increasing amount of the NHS functionalized linker. The degree of labeling was determined by mass spectrometry. A significant amount of Twi remained unlabeled after incubation with only 1 or 2 equiv of **2** relative to Twi. This was partially explained by the fact that the activated ester readily hydrolyzed in aqueous solution after which it would no longer react with amines. However, the size of the linker also appeared to play a role, as more efficient labeling was obtained when smaller molecules with an NHS moiety were used. It was found that the use of 10 equiv of **2** and an incubation time of 2 h at pH 7.5 led to the coupling of one to two linkers per enzyme molecule. The effect of labeling on enzymatic activity was minimal. Modified Twi had retained 85% of its activity compared to the unmodified enzyme.

Altogether, for each enzyme a modification strategy was found which allowed for straightforward and selective introduction of a dibenzocyclooctyne or azide moiety and concomitant conservation of catalytic activity.

Conjugate Formation. As a next step, the conjugate formation was investigated. The assembly of a 4CL-STS-Twi complex was performed in two ways. In the first approach, 4CL-**1** and Twi-**2** were simultaneously added to AHA-STS in equimolar amounts. Upon overnight incubation at room temperature, the reaction mixture was transferred to a size-exclusion column. Whereas nonoligomerized 4CL, Twi, and STS dimer eluted in the same peak after 1.57 mL, the oligomers eluted in two distinguishable peaks at 1.26 and 1.36 mL (see Figure 3A). According to the relative peak areas, the efficiency of conjugate formation was 54%.

The three fractions as indicated in Figure 3A were analyzed by gel electrophoresis (see Figure 3B). The denaturing gel showed that the smallest conjugate fraction (2) contained polypeptides with a mobility corresponding to 100−150 kDa, as well as a considerable amount of free STS. According to a native gel, the free STS was part of the formed complex, suggesting that the conjugates in this fraction mainly consisted of an STS dimer to which one 4CL or Twi molecule was linked. The larger conjugate fraction (1) showed bands above 200 kDa and hardly any monomeric STS. Apparently, the complexes eluting in this fraction contained an STS dimer of which both units were conjugated to at least one 4CL or Twi molecule.

Native mass spectrometry was performed to confirm this hypothesis. Ionization conditions were applied in which the STS dimer stayed intact. A mass of 88.6 kDa was detected in a sample containing AHA-STS only, corresponding to the natural dimeric complex. Conjugation of one 4CL-**1** (61.4 kDa) or one Twi-**2** (55.0 kDa) molecule would result in complexes of 150.0 kDa and 143.6 kDa, respectively. To the set of m/z peaks detected in conjugate fraction (2), different charges could be assigned. The two possibilities leading to the lowest standard deviation in the average mass were those with deconvoluted masses of 151.8 and 145.9 kDa (see Supporting Information Figure S3). This corresponded well with the mass of the 4CL-STS:STS and Twi-STS:STS complexes. With respect to conjugate fraction (1), deconvolution of the detected m/z peaks indicated the presence of complexes with a mass of 214.4,
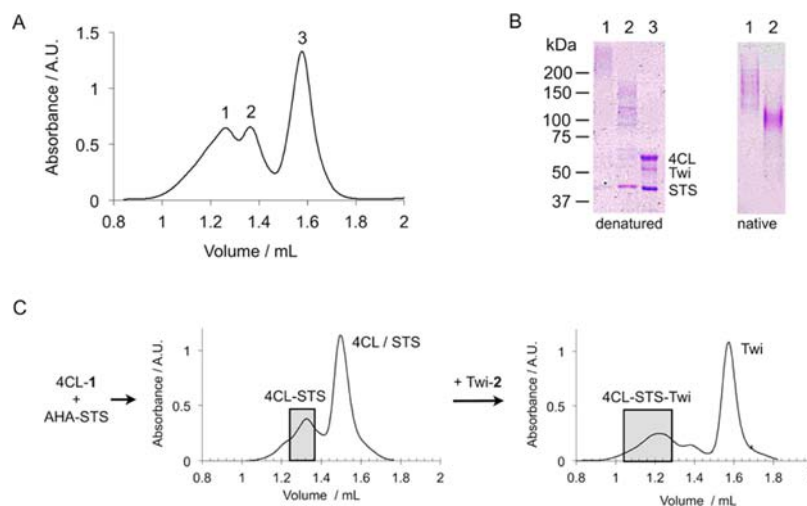
Figure 3. Formation of enzyme oligomers consisting of 4CL-**1**, AHA-STS and Twi-**2**. (A) Size-exclusion chromatogram of enzyme conjugate formation using the one-step approach. Numbers indicate which fractions were collected and analyzed. (B) Denaturing (left) and native (right) 7.5% polyacrylamide gels. The numbers above the lanes correspond with those in the size-exclusion chromatogram displayed in (A). The multiple bands visible between 100 and 150 kDa in lane 2 of the denaturing gel indicate the expected difference in electrophoretic mobility of 4CL-STS and Twi-STS conjugates which are linked at different positions in the polypeptide chains. (C) Formation of enzyme oligomers using a two-step approach. In step 1, 4CL-**1** was reacted with AHA-STS. The gray box in the chromatogram on the left highlights the 4CL-STS conjugate fraction that was collected and used in step 2 in which Twi-**2** was added leading to the formation of the trifunctional complex as highlighted by the gray box in the chromatogram on the right.

208.0, and/or 201.5 kDa. This is in agreement with the masses of the 4CL-STS:STS-4CL, 4CL-STS:STS-Twi, and Twi-STS:STS-Twi assemblies.

Although the one-step strategy resulted in efficient conjugate formation, complex formation consisting of only STS and 4CL or STS and Twi could not be prevented. Therefore, in order to guarantee the formation of trifunctional complexes, the procedure was repeated using a two-step approach. First, 4CL-**1** was allowed to react with AHA-STS in a 1:2 molar ratio. This led to the formation of 4CL-STS:STS conjugates with an efficiency of 30% based on the total protein content. Although this is lower than the 50% of conjugation obtained in the one-step approach, it is in agreement with the fact that in this case two times less 4CL was added compared to STS in order to prevent formation of 4CL-STS:STS-4CL conjugates.

The aliquots containing the STS dimer to which a single 4CL molecule was linked were pooled and mixed with a 3-fold excess of Twi-**2**. The chromatogram obtained after the second size-exclusion step showed a significant amount of protein larger than the 4CL-STS conjugate (see Figure 3C, right). This indicated that the majority of the 4CL-STS conjugate had reacted with Twi-**2** leading to the formation of the trifunctional 4CL-STS-Twi complex. In order to estimate the conjugate formation efficiency in this step, the amount of unreacted Twi was calculated based on the detected peak area at 1.56 mL. By injection of known amounts of Twi a response factor could be calculated, indicating that the peak area at 1.56 mL corresponded to approximately 78 μg of Twi. So, whereas 125 μg of Twi had been added to the conjugation reaction, ~47 μg was coupled to the 4CL-STS:STS complex. Taking into account that a 3-fold molar excess of Twi had been added, this indicated that the conjugate formation had proceeded in quantitative manner based on the amount of 4CL-STS:STS present in the reaction mixture. Native mass spectrometric analysis showed that the remaining protein eluting at 1.4 mL had a smaller mass than the 4CL-STS:STS complex, that is, 135.1 kDa instead of 150.0 kDa. This species, which was

detected in the one-step approach as well, is hypothesized to be an impurity that cannot take part in the conjugate formation. As expected, in the aliquots containing the trifunctional complex a set of m/z peaks was detected that fitted with the expected mass of 205 kDa (see Supporting Information Figure S4). In addition, protein complexes of higher molecular weight were detected, which was explained by the fact that two Twi molecules were coupled to the 4CL-STS:STS conjugate. An alternative explanation could be that part of the isolated conjugate fraction from the first step consisted of 4CL-STS:STS-4CL.

Activity of the Multienzyme Complexes. The ability of the conjugates to catalyze the three-step cascade reaction was monitored in time. 25 μM *para*-coumaric acid, 25 μM coenzyme A, 100 μM malonyl-CoA, 200 μM UDP-glucose, and 0.4−0.8 μM of each enzyme were present in the reaction mixture. These conditions allowed for the detection of resveratrol synthesis and subsequent glycosylation by HPLC (see Figure 4). When compared to a mixture of the three uncoupled enzymes containing the same amount of individual activities, the shapes of the curves were similar. This indicated that the kinetic behavior of the multienzyme complex was
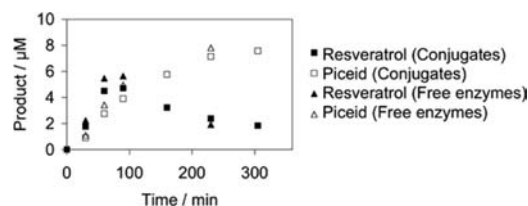

Figure 4. Activity of heteromeric complexes consisting of 4CL, STS, and Twi. The levels of resveratrol and piceid synthesized by the heteromeric complexes, which were formed using the one-step approach, were followed in time and compared to those reached by the nonconjugated enzymes.

comparable to the uncoupled enzymes under the studied reaction conditions.

The effect of conjugation on the individual enzymes was investigated in more detail. In conjugates consisting of STS and Twi or STS and 4CL only, the activity of each enzyme was determined by supplementing the assay mix either with *para*-coumaric acid and coenzyme A, coumaroyl-CoA and malonyl-CoA, or with resveratrol and UDP-glucose. The degree of product formation was compared to the amount of product formed by the unreacted enzymes subjected to the same coupling procedure (see Table 2).

Table 2. Effect of Conjugate Formation on Enzyme Activity[a]

enzyme	complex	% residual activity
4CL	4CL-STS:STS	91
	4CL-STS:STS-4CL	76
STS	Twi-STS:STS	34
	Twi-STS:STS-Twi	17
Twi	Twi-STS:STS	55
	Twi-STS:STS-Twi	32

[a]As compared to the activity of the respective nonreacted enzyme fraction.

■ DISCUSSION

In nature, secondary metabolites, such as isoprenoids, alkaloids, and nonribosomal peptides, are synthesized through multiple reaction steps, which often involve more than two enzymes organized in metabolic complexes. In order to mimic these macromolecular complexes more accurately *in vitro*, it is highly desirable to have access to co-localization strategies for three or more enzymes. Here, we present such a strategy. The application of different modification methods and the use of heterotelechelic linkers enabled us to connect three metabolic enzymes in a defined manner. The two-step approach guaranteed that heteromeric complexes were formed, in which the enzymes with a sequential role in a cascade reaction were covalently coupled to each other in good yield. We show that enzymes derived from different organisms (in this study tobacco, grape, and tomato) can be brought together in one complex and that their activity is retained.

The efficiency of conjugate formation is comparable to values reported elsewhere. For example, the toxin saporin (29 kDa) was covalently linked to the acetyl-functionalized anti-Her2 Fab fragment (50 kDa) using an aminooxy-maleimide linker with 50% coupling efficiency.[20] Moreover, 70% of starting material was consumed in the production of bispecific antibodies using Fab fragments (~50 kDa each) functionalized with either an azide or cyclooctyne moiety.[21] The higher reaction temperature (37 °C) that was used in this study may be an explanation for the slightly higher coupling efficiency. In the synthesis of heterobifunctional protein fusions consisting of hIgG (155 kDa) and either human growth hormone (hGH, 26 kDa) or the maltose-binding protein (MBP, 42 kDa), a conjugation efficiency of 70% was reported as well. In this case, Dibac-functionalized hIgG was allowed to react with a 2-fold excess of azide-functionalized hGH or MBP for 16 h at 4 °C, and the degree of conjugation was based on the density of the IgG protein band in Western blot only.[18]

The influence of complex formation on catalytic activity was found to be largest for STS. This can be explained by the fact that in our assembly approach STS functions as a central assembly point to which both other enzymes are coupled. Therefore, it is most probable that the accessibility to the active site of STS is decreased or its conformation is affected due to linkage of the two other enzymes. This result points out that in order to prevent loss of overall activity, the position of the rate-limiting enzyme should be chosen in such a way that its accessibility is reduced as little as possible. The conjugation process least affected the activity of 4CL. The fact that there is only one point of conjugation in 4CL, located relatively far away from the substrate binding pockets, is seen as the reason for this positive result. It should be noted that 4CL undergoes an 81° interdomain rotation during the catalytic process and that several lysine residues play an essential role in substrate binding.[36] These factors underscore the importance of having control over the site and degree of conjugation.

Contrary to studies reported elsewhere in which enzymes are co-localized by scaffolds, the enzyme conjugates in the present study did not show enhanced product formation. However, this result is in agreement with a study described by Wang et al. in which a 4CL:STS gene fusion and the separate 4CL and STS enzymes showed similar rates for resveratrol synthesis *in vitro*.[37] It was considered to use lower enzyme concentrations or substrate concentrations below the K_m of STS or Twi, because in those cases one should be able to observe the beneficial effect of a local, higher concentration of substrate near the active sites of the enzyme complex. Unfortunately, the high conversion rate of 4CL, the low k_{cat} and K_m of STS and the detection limit of the intermediate and product made it practically impossible to follow the cascade reaction under such conditions.

The enzymes were co-localized without the use of a solid support or supramolecular scaffold. In this way the system is less complex than those in which, for example, enzymes are linked to cellulose *via* cellulose binding domains or are co-immobilized on a DNA template.[10−14] It is an attractive alternative to the production of gene fusions. The proteins are linked after translation and folding at positions different than the N- or C-terminus. In this way, the coupling of more than two biocatalysts is more feasible. Furthermore, our strategy is significantly more selective than the production of combined cross-linked enzyme aggregates using, for example, glutaraldehyde. Therefore, it provides opportunities for the co-localization of less robust enzymes such as the ones applied in the present study.

For comparison, the enzymes were also linked using conventional scaffold-free cross-linking methods. The activities of 4CL and Twi were entirely lost upon incubation with the commonly used nonspecific cross-linker glutaraldehyde. For more controlled two-step conjugation, a commercially available NHS−maleimide cross-linker was tested. When STS was treated with the linker in the first step, a high degree of homo-oligomerization occurred because of the presence of both accessible lysines and cysteines. 4CL could not be used in the first labeling step either because of the presence of an accessible cysteine and the essential role of lysines in the catalytic activity. Finally, also Twi was inactivated when incubated with the NHS−maleimide bifunctional linker. As stated earlier, this can be explained by the presence of a solvent accessible cysteine located at one of the substrate binding regions. These results emphasize the beneficial effect of introducing a non-natural functionality in one of the enzyme candidates. As this functionality is not present in the other enzymes, the undesired formation of homo-oligomers during

the initial functionalization with the heterotelechelic linker is prevented.

Especially in diffusion-limiting medium, co-localization of biocatalysts is expected to be highly beneficial. An example is lignocellulose, a highly viscous material in which the cooperative behavior of multiple cellulases is essential to reach high levels of cellulose degradation for subsequent bioethanol production. From a commercial point of view, the use of low enzyme concentrations is desirable. However, this implies that there is little chance of collaborating enzymes residing in close proximity to each other. A gentle but covalent cross-linking method such as the one presented here is expected to be extremely useful in such an application.

When metabolic enzymes that do not naturally interact would lead to a useful metabolon, the presented approach may be deployed as well. Control over the assembly process, i.e., the relative orientation of the enzymes with respect to each other, may be of particular benefit when a predefined order in conversion is to be maintained. An example is the glycosylation of proteins, which in living cells proceeds in a highly organized manner along the cis and trans Golgi machinery.[38]

Finally, we also expect that the combination of whole-cell biocatalysts and isolated enzymes for application in, for example, the pharmaceutical industry, will profit from an enzyme co-localization strategy such as the one described here. Side-reactions between product intermediates and medium components will be less prone to occur when the isolated enzyme and whole-cell biocatalysts are linked together. Whereas the isolated enzyme can be functionalized *via* genetic engineering to introduce the azide moiety, the whole-cell biocatalyst may be selectively modified *via* natural functionalities occurring at the outside of the cell.

Overall, our approach for the covalent linkage of multiple enzymes using heterotelechelic linkers and the strain-promoted azide−alkyne cycloaddition as bioconjugation reaction is envisioned to be a strategy with high potential for the *in vitro* co-localization of multiple enzymes used in a wide variety of biotechnological applications. When enzyme concentrations are low, diffusion is limited and/or undesired side-reactions have a chance to take place, it will be beneficial to couple the biocatalysts to each other in a mild but irreversible way, thus reaching higher turnover numbers.

■ ASSOCIATED CONTENT

Ⓢ Supporting Information

Synthetic procedures for heterotelechelic linkers **1** and **2**, mass spectrometry protocols, mass spectra of Met-STS, AHA-STS, 4CL, and 4CL-**1** including relevant tryptic fragments (Figure S1 and S2), and of the three-enzyme conjugates (Figures S3 and S4). This material is available free of charge via the Internet at http://pubs.acs.org.

■ AUTHOR INFORMATION

Corresponding Author

*E-mail: j.vanhest@science.ru.nl, phone: +31-24-36-53204, fax: +31-24-36-53393.

Author Contributions

The manuscript was written through contributions of all authors. All authors have given approval to the final version of the manuscript.

Notes

The authors declare no competing financial interest.

■ ABBREVIATIONS

4CL, 4-coumarate:coenzyme A ligase; AHA, azidohomoalanine; CoA, coenzyme A; Dibac, dibenzoazacyclooctyne; Met, methionine; STS, stilbene synthase

■ REFERENCES

(1) Jorgensen, K., Rasmussen, A. V., Morant, M., Nielsen, A. H., Bjarnholt, N., Zagrobelny, M., Bak, S., and Moller, B. L. (2005) Metabolon formation and metabolic channeling in the biosynthesis of plant natural products. *Curr. Opin. Plant Biol. 8*, 280−291.

(2) Winkel, B. S. J. (2004) Metabolic channeling in plants. *Annu. Rev. Plant Biol. 55*, 85−107.

(3) Conrado, R. J., Varner, J. D., and DeLisa, M. P. (2008) Engineering the spatial organization of metabolic enzymes: mimicking nature's synergy. *Curr. Opin. Biotechnol. 19*, 492−499.

(4) Lopez-Gallego, F., and Schmidt-Dannert, C. (2010) Multi-enzymatic synthesis. *Curr. Opin. Chem. Biol. 14*, 174−183.

(5) Zhang, Y. H. P. (2011) Substrate channeling and enzyme complexes for biotechnological applications. *Biotechnol. Adv. 29*, 715−725.

(6) Schoffelen, S., and van Hest, J. C. M. (2012) Multi-enzyme systems: bringing enzymes together in vitro. *Soft Matter 8*, 1736−1746.

(7) Mateo, C., Chmura, A., Rustler, S., van Rantwijk, F., Stolz, A., and Sheldon, R. A. (2006) Synthesis of enantiomerically pure (S)-mandelic acid using an oxynitrilase-nitrilase bienzymatic cascade: a nitrilase surprisingly shows nitrile hydratase activity. *Tetrahedron: Asymmetry 17*, 320−323.

(8) Vafiadi, C., Topakas, E., and Christakopoulos, P. (2008) Preparation of multipurpose cross-linked enzyme aggregates and their application to production of alkyl ferulates. *J. Mol. Catal. B: Enzym. 54*, 35−41.

(9) Scism, R. A., and Bachmann, B. O. (2010) Five-Component Cascade Synthesis of Nucleotide Analogues in an Engineered Self-Immobilized Enzyme Aggregate. *ChemBioChem 11*, 67−70.

(10) Müller, J., and Niemeyer, C. M. (2008) DNA-directed assembly of artificial multienzyme complexes. *Biochem. Biophys. Res. Commun. 377*, 62−67.

(11) Wilner, O. I., Weizmann, Y., Gill, R., Lioubashevski, O., Freeman, R., and Willner, I. (2009) Enzyme cascades activated on topologically programmed DNA scaffolds. *Nat. Nanotechnol. 4*, 249−254.

(12) Dueber, J. E., Wu, G. C., Malmirchegini, G. R., Moon, T. S., Petzold, C. J., Ullal, A. V., Prather, K. L. J., and Keasling, J. D. (2009) Synthetic protein scaffolds provide modular control over metabolic flux. *Nat. Biotechnol. 27*, 753−U107.

(13) You, C., Myung, S., and Zhang, Y. H. P. (2012) Facilitated Substrate Channeling in a Self-Assembled Trifunctional Enzyme Complex. *Angew. Chem., Int. Ed. 51*, 8787−8790.

(14) Fu, J. L., Liu, M. H., Liu, Y., Woodbury, N. W., and Yan, H. (2012) Interenzyme Substrate Diffusion for an Enzyme Cascade Organized on Spatially Addressable DNA Nanostructures. *J. Am. Chem. Soc. 134*, 5516−5519.

(15) Delebecque, C. J., Lindner, A. B., Silver, P. A., and Aldaye, F. A. (2011) Organization of Intracellular Reactions with Rationally Designed RNA Assemblies. *Science 333*, 470−474.

(16) Liu, Y., Du, J., Yan, M., Lau, M. Y., Hu, J., Han, H., Yang, O. O., Liang, S., Wei, W., Wang, H., Li, J., Zhu, X., Shi, L., Chen, W., Ji, C., and Lu, Y. (2013) Biomimetic enzyme nanocomplexes and their use as antidotes and preventive measures for alcohol intoxication. *Nat. Nanotechnol. 8*, 187−92.

(17) You, C., and Zhang, Y. H. P. (2013) Self-Assembly of Synthetic Metabolons through Synthetic Protein Scaffolds: One-Step Purification, Co-immobilization, and Substrate Channeling. *ACS Synth. Biol. 2*, 102−110.

(18) Hudak, J. E., Barfield, R. M., de Hart, G. W., Grob, P., Nogales, E., Bertozzi, C. R., and Rabuka, D. (2012) Synthesis of Heterobifunctional Protein Fusions Using Copper-Free Click Chemistry and the Aldehyde Tag. *Angew. Chem., Int. Ed. 51*, 4161−4165.

(19) Witte, M. D., Cragnolini, J. J., Dougan, S. K., Yoder, N. C., Popp, M. W., and Ploegh, H. L. (2012) Preparation of unnatural N-to-N and C-to-C protein fusions. *Proc. Natl. Acad. Sci. U. S. A. 109*, 11993−11998.

(20) Hutchins, B. M., Kazane, S. A., Staflin, K., Forsyth, J. S., Felding-Habermann, B., Smider, V. V., and Schultz, P. G. (2011) Selective Formation of Covalent Protein Heterodimers with an Unnatural Amino Acid. *Chem. Biol. 18*, 299−303.

(21) Kim, C. H., Axup, J. Y., Dubrovska, A., Kazane, S. A., Hutchins, B. A., Wold, E. D., Smider, V. V., and Schultz, P. G. (2012) Synthesis of Bispecific Antibodies using Genetically Encoded Unnatural Amino Acids. *J. Am. Chem. Soc. 134*, 9918−9921.

(22) Jang, M. S., Cai, E. N., Udeani, G. O., Slowing, K. V., Thomas, C. F., Beecher, C. W. W., Fong, H. H. S., Farnsworth, N. R., Kinghorn, A. D., Mehta, R. G., Moon, R. C., and Pezzuto, J. M. (1997) Cancer chemopreventive activity of resveratrol, a natural product derived from grapes. *Science 275*, 218−220.

(23) Baur, J. A., and Sinclair, D. A. (2006) Therapeutic potential of resveratrol: the in vivo evidence. *Nat. Rev. Drug Discovery 5*, 493−506.

(24) Beekwilder, J., Wolswinkel, R., Jonker, H., Hall, R., de Vos, C. H. R., and Bovy, A. (2006) Production of resveratrol in recombinant microorganisms. *Appl. Environ. Microbiol. 72*, 5670−5672.

(25) Watts, K. T., Lee, P. C., and Schmidt-Dannert, C. (2006) Biosynthesis of plant-specific stilbene polyketides in metabolically engineered Escherichia coli. *BMC Biotechnol. 6*, 22−33.

(26) Becker, J. V. W., Armstrong, G. O., Van der Merwe, M. J., Lambrechts, M. G., Vivier, M. A., and Pretorius, I. S. (2003) Metabolic engineering of Saccharomyces cerevisiae for the synthesis of the wine-related antioxidant resveratrol. *FEMS Yeast Res. 4*, 79−85.

(27) Zhang, Y. S., Li, S. Z., Li, J., Pan, X. Q., Cahoon, R. E., Jaworski, J. G., Wang, X. M., Jez, J. M., Chen, F., and Yu, O. (2006) Using unnatural protein fusions to engineer resveratrol biosynthesis in yeast and mammalian cells. *J. Am. Chem. Soc. 128*, 13030−13031.

(28) Shimoda, K., Kondo, Y., Nishida, T., Hamada, H., Nakajima, N., and Hamada, H. (2006) Biotransformation of thymol, carvacrol, and eugenol by cultured cells of Eucalyptus perriniana. *Phytochemistry 67*, 2256−2261.

(29) Ibern-Gomez, M., Roig-Perez, S., Lamuela-Raventos, R. M., and de la Torre-Boronat, M. C. (2000) Resveratrol and piceid levels in natural and blended peanut butters. *J. Agric. Food Chem. 48*, 6352−6354.

(30) Hollman, P. C. H. (2004) Absorption, bioavailability, and metabolism of flavonoids. *Pharm. Biol. 42*, 74−83.

(31) Schoffelen, S., Lambermon, M. H. L., van Eldijk, M. B., and van Hest, J. C. M. (2008) Site-specific modification of Candida antarctica lipase B via residue-specific incorporation of a non-canonical amino acid. *Bioconjugate Chem. 19*, 1127−1131.

(32) Kramer, G., Sprenger, R. R., Back, J., Dekker, H. L., Nessen, M. A., van Maarseveen, J. H., de Koning, L. J., Hellingwerf, K. J., de Jong, L., and de Koster, C. G. (2009) Identification and Quantitation of Newly Synthesized Proteins in Escherichia coli by Enrichment of Azidohomoalanine-labeled Peptides with Diagonal Chromatography. *Mol. Cell. Proteomics 8*, 1599−1611.

(33) Thanbichler, M., Neuhierl, B., and Bock, A. (1999) S-methylmethionine metabolism in Escherichia coli. *J. Bacteriol. 181*, 662−665.

(34) Austin, M. B., Bowman, M. E., Ferrer, J. L., Schroder, J., and Noel, J. P. (2004) An aldol switch discovered in stilbene synthases mediates cyclization specificity of type III polyketide synthases. *Chem. Biol. 11*, 1179−1194.

(35) Debets, M. F., van Berkel, S. S., Schoffelen, S., Rutjes, F. P. J. T., van Hest, J. C. M., and van Delft, F. L. (2010) Aza-dibenzocyclooctynes for fast and efficient enzyme PEGylation via copper-free (3 + 2) cycloaddition. *Chem. Commun. 46*, 97−99.

(36) Hu, Y. L., Gai, Y., Yin, L., Wang, X. X., Feng, C. Y., Feng, L., Li, D. F., Jiang, X. N., and Wang, D. C. (2010) Crystal Structures of a Populus tomentosa 4-Coumarate:CoA Ligase Shed Light on Its Enzymatic Mechanisms. *Plant Cell 22*, 3093−3104.

(37) Wang, Y. C., Yi, H., Wang, M., Yu, O., and Jez, J. M. (2011) Structural and Kinetic Analysis of the Unnatural Fusion Protein 4-Coumaroyl-CoA Ligase::Stilbene Synthase. *J. Am. Chem. Soc. 133*, 20684−20687.

(38) Schoberer, J., and Strasser, R. (2011) Sub-Compartmental Organization of Golgi-Resident N-Glycan Processing Enzymes in Plants. *Mol. Plant 4*, 220−228.